Contents lists available at ScienceDirect

EBioMedicine

Research paper

Interleukin-24 protects against liver injury in mouse models

Hsiao-Hsuan Wang[a], Jian-Hao Huang[b], Min-Hao Sue[b], Wei-Chih Ho[b], Yu-Hsiang Hsu[c,d], Kung-Chao Chang[e], Ming-Shi Chang[a,b,*]

[a] Institute of Basic Medical Sciences, College of Medicine, National Cheng Kung University, Tainan, Taiwan
[b] Department of Biochemistry and Molecular Biology, College of Medicine, National Cheng Kung University, Tainan, Taiwan
[c] Institute of Clinical Medicine, College of Medicine, National Cheng Kung University, Tainan, Taiwan
[d] Research Center of Clinical Medicine, National Cheng Kung University Hospital, Tainan, Taiwan
[e] Department of Pathology, National Cheng Kung University Hospital, College of Medicine, National Cheng Kung University, Tainan, Taiwan

ARTICLE INFO

ABSTRACT

Background: Interleukin-24 (IL-24) binds to two kinds of receptor complexes, namely IL-20R1/IL-20R2 and IL-20R2/IL-22R1, which are also bound by IL-20. IL-20 plays a detrimental role in liver fibrosis. Due to the sharing of receptor complexes, we aimed to determine whether IL-24 also participates in liver fibrosis.
Methods: Clinical biopsy specimens from various stages of liver fibrosis were used to analyze IL-24 expression. IL-24 protein was administered to mice with thioacetamide (TAA)-induced liver injury. The direct effects of IL-24 on mouse primary hepatocytes or hepatic stellate cells (HSCs) were analyzed. Wild-type, IL-20R1-, and IL20R2-deficient mice were used to establish a model of acute TAA-induced liver injury.
Findings: Among patients with more severe liver fibrosis, there was a reduced IL-24/IL-20 ratio. Administration of IL-24 protein protected mice from TAA-induced liver injury and reduction of liver inflammation by antioxidant effects. IL-24 protected hepatocytes from TAA-induced apoptosis and prevented liver fibrosis through the inhibition of the HSCs activation. The protective role of IL-24 acted on liver cells were mainly IL-20R1-independent. IL-20R2-deficient mice exhibited more severe liver injury upon TAA treatment, thus confirming the protective role of IL-24.
Interpretation: IL-24 plays a key protective role in the progression of liver injury and has therapeutic potential for treating liver injuries.
Funding: This work was supported by the Ministry of Science and Technology of Taiwan (MOST 106−2320-B-006−024) and Taiwan Liver Disease Prevention & Treatment Research Foundation.

1. Introduction

Liver fibrosis is defined as the excessive extracellular matrix (ECM) deposition when encountering injuries [1,2]. In response to various stimuli, such as drugs or toxic compounds, alcohol abuse, and metabolic disorders [3,4], the fibrosis process occurs in several types of cells, including hepatocytes, Kupffer cells, monocytes, and stellate cells. Under stress conditions, the damaged hepatocytes produce reactive oxygen species (ROS), several inflammatory mediators, and fibrogenic factors to send signals to surrounding cells [5]. After receiving the signals, the activated Kupffer cells and the infiltrated Ly6C+ monocytes play important roles in liver inflammation and fibrotic response [6-10].

The fibrosis factor-transforming growth factor (TGF)-β secreted by damaged liver cells is the most prominent driver for the activation of quiescent hepatic stellate cells (HSC) [11,12]. Activated HSCs upregulate the expression of α-smooth muscle actin (α-SMA) and proliferate and secret other pro-fibrotic mediators, including tissue inhibitors of metalloproteinases (TIMPs) and alpha-1 type I collagen (COL-1 -A1) [13,14]. Excessive deposition of ECM produced by proliferating activated HSCs leads to fibrosis and cirrhosis [15]. When such injury is prolonged, hepatocellular carcinoma (HCC) may even develop.

Interleukin-24 (IL-24), together with IL-19, IL-20, IL-22, and IL-26, is a member of the IL-20 subfamily, and they have the same receptor subunits [16]. IL-24 signaling occurs through two kinds of heterodimeric receptor complexes, including IL-20R1/IL-20R2 and IL-20R2/IL-22R1, which are shared with IL-20 [17,18]. The pro-inflammatory cytokine interleukin-20 (IL-20) reportedly played an important role in the pathogenesis of liver fibrosis [19]. During the fibrotic process, IL-20 was secreted by damaged hepatocytes, which further triggered

Research in Context

Evidence before this study

Liver diseases like hepatic fibrosis and cirrhosis are important causes of morbidity and mortality worldwide. The pro-inflammatory cytokine interleukin-20 (IL-20) reportedly played a detrimental role in liver fibrosis. Interleukin-24 (IL-24), which shares the same receptor complexes with IL-20, was shown to be a tumor suppressor previously. However, the role IL24 plays in the liver injury process was unknown.

Added value of this study

Through the analysis of the clinical liver biopsies, in patients with lower IL-24 protein levels, the fibrosis score is higher. IL-24 protein treatment protects mice from toxin-induced acute and chronic liver injury by reducing the area of the damaged liver, improving liver function, and suppressing liver inflammation. IL-24 protects against liver fibrosis by blocking the activation and proliferation of hepatic stellate cells. IL-24 and IL-20 prefer to use different receptor complexes to have opposite effects on liver cells. The deficient of the IL-24 signaling causes severe liver damage in a toxin-induced liver injury model.

Implications of all the available evidence

Our findings indicate that IL-24 has hepatoprotective effects and anti-fibrotic properties, providing a potential drug candidate for the treatment of liver diseases.

the activation of HSCs and increased the expression of TGF-β [19]. Therefore, we hypothesized that IL-24, which shares the same receptor complexes as IL-20, may also participate in the liver injury process. We aimed to explore the role of IL-24 in liver fibrosis using clinical samples from patients with liver diseases and thioacetamide (TAA)-induced liver injury model.

2. Methods

2.1. Clinical specimens

Liver biopsies were taken from 25 patients with various liver diseases between January 1991 and January 2019 (non-fibrosis, n = 4; moderate chronic active hepatitis, n = 7; severe chronic active hepatitis, n = 7; cirrhosis, n = 7). This retrospective study was approved by the National Cheng Kung University Hospital Institutional Review Board (IRB No: A-ER-108−439). Biopsies were taken after obtaining informed consent from 25 participants. Detailed information about the clinical specimens was listed in Supplementary Table S1. The clinicopathological variables evaluated were listed in Supplementary Table S2−3. The fibrosis scores and METAVIR scores in the patients with non-fibrosis, moderate hepatitis, severe hepatitis, and cirrhosis were analyzed (Figure S4a).

2.2. Immunofluorescence (IF)

The locations of IL-24 and IL-20 in liver biopsies obtained from patients with various liver diseases were assessed by IF staining. Tissues were fixed in 4% paraformaldehyde solution, proceed with dehydration, and embedding according to common methods by Human Biobank in National Cheng Kung University Hospital. Paraffin-embedded tissue sections (4 μm) were deparaffinized, rehydrated, and subjected to heat-induced antigen retrieval by Tris-EDTA buffer (10 mM Tris base, 1 mM EDTA solution, 0•05%Tween 20, pH8•5) for 95 °C

30 min. Nonspecific binding was blocked by treatment with blocking reagent (Thermo Fisher Scientific Cat# 003118). The sections were incubated with anti-IL-24 antibody (Thermo Fisher Scientific Cat# MA5-27141, RRID:AB_2723287) or anti-IL-20 antibody (7E) at 4 °C overnight. 7E was prepared as previously described [20]. Anti-$\alpha-$SMA (Abcam Cat# ab124964, RRID:AB_11129103) was used as a marker for activated HSCs, while anti-HNF-4 (Abcam Cat# ab201460) was served as the marker of hepatocytes. At the second day, they were incubated for 1 h with Alexa Fluor®488-conjugated anti-mouse secondary antibody (Jackson ImmunoResearch Labs Cat# 115−545−003, RRID:AB_2338840) and Alexa Fluor®594-conjugated anti-rabbit secondary antibody (Jackson ImmunoResearch Labs Cat# 111-585-003, RRID:AB_2338059), and finally mounted with DAPI (Vector Laboratories Cat# H-1200, RRID:AB_2336790). Anti-cleaved Caspase-3 antibody (Cell Signaling Technology Cat# 9661, RRID: AB_2341188) was used to analyze the apoptotic cells in AML12 cells. We applied IF staining to analyze the expression levels of the activated HSCs marker − $\alpha-$SMA (Abcam Cat# ab124964, RRID: AB_11129103).

2.3. Immunohistochemistry (IHC)

Paraffin sections (4 μm) of liver biopsies obtained from non-fibrosis (n = 4), patients with moderate hepatitis (n = 7), severe hepatitis (n = 7), and cirrhosis (n = 7) were used for IHC staining with the anti-IL-24 antibody (Thermo Fisher Scientific Cat# MA5−27141, RRID: AB_2723287) and the anti-IL-20 antibody (7E). Sections incubated with mIgG isotype (R and D Systems Cat# MAB002, RRID: AB_357344) were used as negative control. The protein expression of IL-24 and IL-20 was quantified by HistoQuest (TissueGnostics) as mean intensity (pixel). IHC staining was performed to analyze the expression levels of IL-24, IL-20, IL-20R1, IL-20R2, IL-22R1, F4/80, TGF-β, and $\alpha-$SMA in the mice liver. Briefly, paraffin sections were incubated with primary antibody against IL-24 (R and D Systems Cat# AF2786, RRID:AB_2124803), IL-20 (7E), IL-20R1 (Abcam Cat# ab203196, RRID:AB_2750843), IL-20R2 (Abcam Cat# ab95824, RRID: AB_10678407), IL-22R1 (Abcam Cat# ab5984, RRID:AB_305220), F4/80 (Cell Signaling Technology Cat# 70076, RRID:AB_2799771), TGF-β (Proteintech Cat# 18978-1-AP, RRID:AB_11182379), and $\alpha-$SMA (Abcam Cat# ab124964, RRID:AB_11129103) 4 °C overnight. The next day, the sections were washed with PBS and incubated with the secondary antibody for one hour. The reaction was detected using AEC chromogen stain (ScyTek Laboratories Cat# ACG500), and the nuclei was counterstained with hematoxylin (ScyTek Laboratories Cat# HMM500).

2.4. Animal experiments

6−8 weeks old C57BL/6 JNarl wild-type male mice (weighing 20−25 g) were purchased from Taiwan National Laboratory Animal Center. All animals were kept on a 12 h light-dark cycle at 22 ± 2 °C and experiments were conducted according to the protocols based on the National Institutes of Health standards and guidelines for the care and use of experimental animals. The research procedures were approved by the Animal Ethics Committee of Taiwan National Cheng Kung University (IACUC Approval No: 105087). Every effort was made to minimize animal suffering and to reduce the number of animals used. A total of 154 mice were used in this study. All animals analyzed were included in the results and none was excluded. The sample size for each animal experiment was determined by past experience, usually with 5 animals per group in each experiment. Mice were randomized before starting treatment in all experiments. The students who were responsible for the allocation and the conduct of the experiment were different from those performing the outcome assessment and the data analysis.

Short-term acute liver injury was established by a single intraperitoneal injection of thioacetamide (TAA; Sigma-Aldrich Cat# 163678) (150 mg/kg of body weight). For IL-24-pre-treatment experiment (n=5 per experimental group, a total of 15 mice were used in the experiment), recombinant mouse IL-24 protein (1 mg/kg) or PBS was intraperitoneally injected into mice 24 h before TAA treatment followed by another two injections of IL-24 at 24th and 48th hour after TAA treatment. Mice were sacrificed 72 h after TAA treatment. For the therapeutic experiment, mice were randomly given PBS or recombinant mouse IL-24 protein (1•5 mg/kg) at 24 h and 48 h after TAA treatment (n=3 per experimental group, a total of 9 mice were used in the experiment). Mice were sacrificed 72 h after TAA treatment.

In the long-term study, mice were intraperitoneally injected with 100 mg/kg TAA three times a week for 8 weeks. Mice were also treated with PBS or mIL-24 (1•5 mg/kg) twice a week from week 4 to week 8 (n=5 per experimental group, a total of 15 mice were used in the experiment). Mice were sacrificed at week 8. Liver from sacrificed animals were immediately frozen in liquid nitrogen or were preserved in 4% paraformaldehyde solution and processed in paraffin tissue-processing method according to common methods by Human Biobank in National Cheng Kung University Hospital. Hematoxylin and eosin stain (H&E stain) and Sirius red stain were applied to analyze liver damage and the deposition of collagen. IL-20R2-deficient mice were generated and were backcrossed into C57BL/6 genetic background for at least six generations (Figure S1a). A PCR genotyping method was used to distinguish wild-type and IL-20R2-deficient mice (Figure S1b). In the animal model of short-term TAA-induced acute liver injury, the male wild-type mice, IL-20R1-, and IL-20R2-deficient mice used in this study were between 8 and 10 weeks old (n = 5 per experimental group, a total of 30 mice were used in the experiment).

2.5. Sample collection and serum biochemistry

Blood was collected via retro-orbital sinus puncture or cardiac puncture. Serum was frozen at −80 °C for the analysis of aspartate transaminase (AST), alanine aminotransferase (ALT), bilirubin with an automatic biochemical analyzer (Olympus).

2.6. Terminal deoxynucleotidyl transferase dUTP nick end labeling (TUNEL) assay

Liver paraffin sections from mice were deparaffinized and rehydrated. The apoptotic cells were detected by staining with Dead-End™ Fluorometric TUNEL System (Promega Cat# G3250).

2.7. Real-time PCR

Total RNA was extracted from frozen liver samples using Trizol reagent (Sigma Cat# T9424) and reverse transcription was performed with reverse transcriptase (PrimeScript RT-PCR kit) according to the manufacturer's protocol. The expression levels of *Tnfa, Il20, Il24, Tgfb, Ly6c, Sod, Gpx1, Cat, Bax, Bcl2, Col1a1, Acta2, Timp2, Il20r1, Il20r2, Il22r1, Gfap, Pcna, Cxcl1,* and *Cxcl3* were amplified on a StepOnePlus™, with SYBR Green (Applied Biosystem) for quantitative analysis normalized with Glyceraldehyde phosphate dehydrogenase (*Gapdh*), as internal control. Relative multiples of change in mRNA expression were determined by calculating $2^{-\Delta\Delta CT}$. All primers were synthesized by Genemessenger Co., Ltd., Taiwan. The sequence and the melting temperature of each primer used in this study is listed in Supplementary Table S4.

2.8. Expression and purification of mouse IL-24

Mouse *Il24* mRNA was isolated from murine HCC ML-14a cell line (The Food Industry Research and Development Institute, Taiwan).

Mouse *Il24* was amplified with PCR using gene-specific forward and reverse primers. The amplified PCR fragment coding from Gln-to Leu (aa 27−181) was inserted into the *E.coli* expression vector of pET22b (Invitrogen). The recombinant plasmid pET22b-*Il24* was transformed into BL21 (DE3) pLysS competent cells (Life Technologies). The competent cells was inoculated into 20 ml terrific broth (TB; Sigma-Aldrich) medium, incubated at 37 °C 12 h with shaking at 250 rpm. Then the bacterial culture were amplified into 1 L TB (1:100) and incubated at 37 °C 3 h with shaking at 250 rpm. When the OD600 of the cultured medium reached 0•6, the culture was induced with IPTG (Promega) at a final concentration of 1 mM for 3 h. The enriched inclusion body was re-suspended and passed through the Q column (GE Healthcare). The flow-through was collected and filtrated through a 0•22-μm Millipore filter (Millipore). Protein expression was analyzed by SDS-PAGE (16% separating gel and 4% stacking gel) and western blot (Figure S2).

2.9. Isolation of primary hepatic stellate cells and hepatocytes

We isolated the primary hepatic stellate cells from male C57BL/6 JNarl wild-type mice, IL-20R1-, and IL-20R2-deficient mice (a total of 18 mice were used in the experiment) through the perfusion of the digestive enzymes including pronase E and collagenase P according to the protocol previously described [21]. Primary hepatic stellate cells were characterized by the auto-fluorescent vitamin A-containing vacuoles phenotype. In addition, α-SMA staining (Figure S3) was also available on primary HSCs on day7. Primary hepatocytes were isolated from C57BL/6 JNarl male wild-type, IL-20R1-, and IL-20R2-deficient mice (a total of 9 mice were used in the experiment) through collagenase perfusion procedure. Briefly, mice were anesthetized and perfused with Hank's Balanced Salt Solution (HBSS) containing collagenase type IV. Percoll solution was also applied to isolate the primary hepatocytes.

2.10. Cell experiments

AML12 cell line (ATCC CRL-2254) (RRID: CVCL_0140) was originally purchased from American Type Culture Collection (Manassas, VA). The rat hepatic stellate cell line HSC-T6 (Sigma Cat# SCC069) was purchased from Sigma-Aldrich. AML12 cells were culture in DMEM/F12 medium supplemented with 10%FBS, 2 mM glutamine, penicillin/streptomycin, 1% non-essential amino acid, 1% insulin-transferrin-selenium and 0•1 μM dexamethasone. For TAA-induced apoptosis experiment, AML12 were seeded in 6 well and starvation for 12−16 h, then treated with H_2O or TAA (100 mM)+PBS or TAA (100 mM)+IL-24 (400 ng/ml) for 24 h. For knockdown experiment, PBS or IL-24 (400 ng/ml) or IL-20 (400 ng/ml) were added to shScramble, shIL-20R2, and shIL-22R1 cells for 6 h.

HSC-T6 cells were growth in DMEM/HG supplemented with 10%FBS and penicillin/ streptomycin. Cell proliferation of the HSC-T6 was assessed by the MTT assay. Briefly, cells were replaced with serum-free medium for 16 h and then treated with PBS or rat IL-24 protein (400 ng/ml) (LSBio Cat# LS-G14689), the MTT reagent (Sigma Cat# 475989) was added after 24, 48, and 72 h. Two hours after the addition of MTT reagent, the MTT formazan was dissolved in DMSO (JT Baker Cat# 9224−01) and measured at OD550 nm. We defined the OD550 nm at the 24th hour as 100% in the PBS and IL-24 groups, and then calculated the numbers of cell growth at 48th hour and 72nd hour respectively.

2.11. RNA interference

AML12 cells were infected with VSV-G pseudotyped lentivirus containing Scramble shRNA, IL-20R2 shRNA, and IL-22R1 shRNA at a multiplicity of infection (MOI) of 50. The next day, cells were selected

by puromycin with a concentration of 4 μg/ml. The sequences of the shRNAs are given in Supplementary Table S5.

2.12. Measurement of the catalase activity

The frozen liver tissue was homogenized in cold 1xPBS and centrifuged at 4 °C 12,000 rpm for 10 min. The supernatant was used to measure the activity of catalase by evaluating the rate of degradation of H_2O_2 according to the previous study [22].

2.13. Statistical analysis

Statistical analysis was performed using GraphPad Prism version 6 (GraphPad Software, USA). The experimental data are presented as the mean $\pm$ SEM. GraphPad Prism software is used to process initial data and graphs. The comparison between the two groups was analyzed by unpaired two-sided Student's t-test. One-way ANOVA analysis was used to compare data among groups in experiments including three or more groups. $p < 0.05$ was considered significant (* $p < 0.05$, ** $p < 0.01$, *** $p < 0.001$, and **** $p < 0.0001$). All data were collected in Microsoft Excel and GraphPad Prism 6.

2.14. Role of funding source

3. Results

3.1. The ratio of IL-24/IL-20 was decreased significantly with more severe liver fibrosis

To investigate the clinical correlation of IL-24 with liver fibrosis, we analyzed the expression levels of IL-24 in the liver biopsies from patients with liver disease. Immunofluorescence staining showed IL-24 was not expressed in the α-SMA-positive area (Fig. 1a). However, IL-24 was strongly expressed at the region surrounding the marker of hepatocytes, HNF-4 (hepatocyte nuclear factor-4) (Fig. 1b), it indicated IL-24 was mainly expressed in hepatocytes, but not expressed in the fibrotic area. In contrast, IL-20 was strongly expressed in the α-SMA-positive area (Fig. 1c), which was mainly consisted of the activated hepatic stellate cells (HSCs). IL-20 was not expressed in the HNF-4-positive area (Fig. 1d). IL-24 expression was higher in the non-fibrotic liver and decreased with increasing disease severity (Fig. 1e and 1f). However, IL-20 was weakly expressed in the non-fibrotic liver and increased as fibrosis became more severe (Fig. 1e and 1g). IL-24/IL-20 ratio was significantly decreased when the liver disease become more severe (Fig. 1h). The fibrosis score and META-VIR score in patients with various liver diseases were also analyzed (Figure S4a). In patients with higher IL-24 level or the IL-24/IL-20 ratio, the fibrosis score and the METAVIR score were lower (Figure S4b). Furthermore, we analyzed the levels of the receptors, including IL-20R1, IL-20R2, and IL-22R1 in non-fibrosis and cirrhosis groups (Figure S5). Both IL-20R1 and IL-20R2 were strongly upregulated in cirrhotic liver. However, IL-22R1 was downregulated in the cirrhosis group compared to non-fibrosis group.

3.2. IL-24 administration protected mice from acute liver injury

To investigate the role of IL-24 in the liver injury process, we analyzed the effects of IL-24 on the disease model of acute liver injury. In the IL-24-pretreatment short-term acute liver injury experiment, all mice were sacrificed 72 h after TAA treatment. The TAA+IL-24 group showed a reduction of the damaged area in liver compared to that of the TAA+PBS group via H&E stain (Fig. 2a). IL-24 was decreased after

TAA treatment (Fig. 2b). However, IL-20 was upregulated in the TAA +PBS group and was inhibited after IL-24 treatment (Fig. 2c). The protein level of TGF-β was also downregulated in the TAA+IL-24 group (Fig. 2d). After TAA treatment, the level of *Il24* was decreased, while *Il20* was upregulated in the liver (Fig. 2e), the activities of which was reversed after treatment with IL-24. The gene expression of pro-inflammatory factors— *Tnfa, Cxcl1, Cxcl3*, and fibrogenic factors including *Tgfb* and *Ly6c* were also significantly downregulated in the liver of the IL-24-treated mice (Fig. 2e). Further, TAA may promote the inflammation through the NF-$_K$B pathway during the liver injury process, and IL-24 reduced the phosphorylation of NF-$_K$B in the mice model (Figure S6). IL-24 treatment also ameliorated liver damage by promoting the expression of genes involved in antioxidant reactions like *Sod* and *Gpx1* and reducing cell death (*Bax/Bcl2*) (Fig. 2e). TUNEL assay showed IL-24 significantly protected liver cells from TAA-induced apoptosis in mouse model (Fig. 2f). We also used *in vitro* experiments to analyze the effects of IL-24 on TAA induced-AML12 hepatocyte apoptosis. AML12 hepatocytes express IL-20R1, IL-20R2, and IL-22R1 subunits, thus, they were potential targets for IL-24 or IL-20 (Figure S7a). IL-24 treatment significantly inhibited IL-20 expression (Figure S7b-c). IL-24 treatment protected AML12 hepatocytes from TAA-induced apoptosis (Fig. 2g). IL-24 also protected liver cells by enhancing the activity of catalase in animal model (Fig. 2h). These results suggested that IL-24 potentially prevents liver damage by protecting hepatocytes from cell death and blocks the inflammatory response.

To prove that IL-24 has therapeutic potential, we wanted to prove that IL-24 also had efficacy in protection after the liver was injured. We treated mice with IL-24 protein after TAA treatment. We observed that the liver was severely injured 24 h after TAA treatment based on H&E stain (Figure S8). Therefore, mice were treated with IL-24 protein 24 h after TAA injection to determine the effect of IL-24 on acute liver injury. IL-24-treated mice showed protection against liver injury, loss of liver function (AST, ALT), and the expression of fibrogenic factor and inflammatory factor (Figure S9). Therefore, IL-24 also had a therapeutic effect after the liver had been injured.

3.3. IL-24 protein-treated mice were resistant to chronic liver injury

To analyze the effects of IL-24 on long-term TAA-induced chronic liver injury, treatment with IL-24 was initiated at the 4th week after TAA treatment when the liver fibrosis had occurred. Serum levels of AST and ALT were downregulated in the TAA+IL-24 group compared to those in the TAA+PBS group after the 5−6th week (Fig. 3a). All mice were sacrificed at the 8th week. Sirius red staining was applied to visualize collagen fibers (Fig. 3b). The collagen fibers were reduced after the treatment with IL-24. Similar to the results in the short-term liver injury model, long-term TAA-induced chronic liver damage can also lead to a decrease in IL-24 and an increase in IL-20 (Fig. 3c-d). The protein marker of the activated HSCs, α-SMA, in liver tissue was also reduced after IL-24 treatment (Fig. 3e). In addition, the amount of the F4/80-positive macrophages was reduced in the TAA-IL-24 group, indicating the liver inflammation is improved (Fig. 3f). The mRNA expression of pro-inflammatory factor, fibrogenic factors and antioxidant gene including *Acta2, Col1a1, Tgfb, Tnfa, Ly6c, Timp2*, and *Cat* were ameliorated in the IL-24-treated group (Fig. 3g). The activity of catalase in the liver was also maintained in the TAA +IL-24 group (Fig. 3h). These results demonstrated that IL-24 protected against liver injuries after fibrosis occurred in the chronic fibrosis model. Also, we found IL-20R1 and IL-20R2 were upregulated in the fibrotic liver, however, IL-22R1 was downregulated (Figure S10a), the pattern was similar to that of clinical biopsies (Figure S5). Through the *in vitro* cell experiments, IL-24 not only inhibited the gene expression of *Il20* but also promoted the expression of itself, *Il20r2*, and *Il22r1* (Figure S7b-c, S10b). While IL-20 was unable to
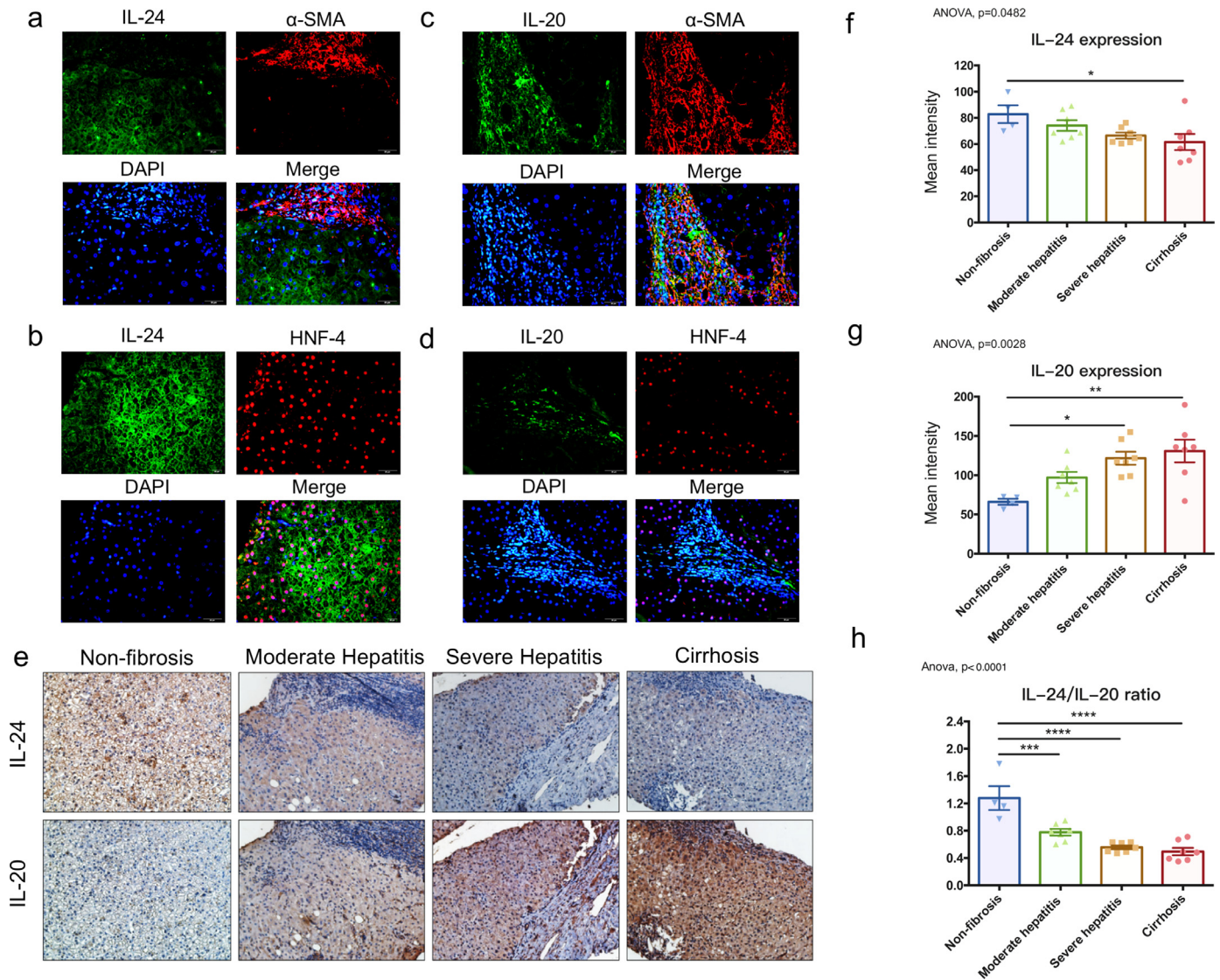
Fig. 1. IL-24 expression was decreased when the disease severity in patients was more serious. Immunofluorescence staining of (a) IL-24 (green) and α-SMA (red) in liver section of a patient with severe hepatitis. Nuclei were stained with DAPI (blue). Original magnification: 400 × . (b) IL-24 (green) and HNF-4 (red) in liver section of a patient with moderate hepatitis. Nuclei were stained with DAPI (blue). Original magnification: 400 × . (c) IL-20 (green) and α-SMA (red) in liver sections of patients with severe hepatitis. Nuclei were stained with DAPI (blue). Original magnification: 400 × . (d) IL-20 (green) and HNF-4 (red) in liver section of a patient with moderate hepatitis. Nuclei were stained with DAPI (blue). Original magnification: 400 × . (e) Paraffin sections of liver biopsies were obtained from subjects without fibrosis (n = 4) and patients with moderate hepatitis (n = 7), severe hepatitis (n = 7), and cirrhosis (n = 7). IL−24 and IL-20 were detected using immunohistochemistry. The reaction was detected using AEC chromogen stain (red), and the nuclei were counterstained with hematoxylin (blue). The figure was representative of 25 samples. Original magnification: 200 × . (f) The protein expression levels of IL-24 in liver biopsies were quantified by HistoQuest and are presented as mean intensity (pixels). One-way ANOVA, $p = 0\bullet0482$; * $p < 0\bullet05$. (g) The level of IL-20 was also quantified by HistoQuest as mean intensity (pixels). One-way ANOVA, $p = 0\bullet0028$; * $p < 0\bullet05$, ** $p < 0\bullet01$. (h) The IL-24/IL-20 ratio in patients with various liver diseases. One-way ANOVA, $p < 0\bullet0001$; *** $p < 0\bullet001$, **** $p < 0\bullet0001$. Data are means ± SEM.

suppress the gene expression of *Il24*, it only upregulated itself, *Il20r1*, and *Il20r2* (Figure S7c, S10c). Therefore, IL-24 is an upstream regulator in modulating several factors including IL-20 during liver fibrosis process.

3.4. IL-24 was downregulated upon activation of hepatic stellate cells

Since HSCs activation is a very crucial step for the initiation of fibrosis, we further investigated the dynamic expression profiles of IL-24 and IL-20 during HSCs activation. We isolated primary HSCs from wild-type male mice for cell culture. On the following days, HSCs began to differentiate into activated HSCs with a myofibroblast-like phenotype. We found the activated HSCs expressed α-SMA on day 7 as previously reported [21] (Figure S3). Hence, we harvested the mRNA of the primary HSCs on days 1, 3, 5, and 7. During HSCs

activation, glial fibrillary acidic protein (*Gfap*), a quiescent HSCs marker, was downregulated (Fig. 4a), while *Acta2* (also called as α-SMA), an activated HSCs marker, and alpha-1 type I collagen (*Col1a1*) were gradually upregulated (Fig. 4a). *Il24* was initially upregulated on day 3 but was markedly downregulated upon activation of HSCs (Fig. 4b). In contrast, *Il20* was upregulated with time upon HSCs activation (Fig. 4b). These results indicated that quiescent HSCs had higher levels of *Il24* and lower levels of *Il20* than the activated HSCs. During HSCs activation, *Il24* was downregulated, while *Il20* was continuously upregulated.

3.5. IL-24 inhibited the marker of activated hepatic stellate cells

Given that activated HSCs are the main source of ECM production for liver fibrosis, we explored whether IL-24 protected
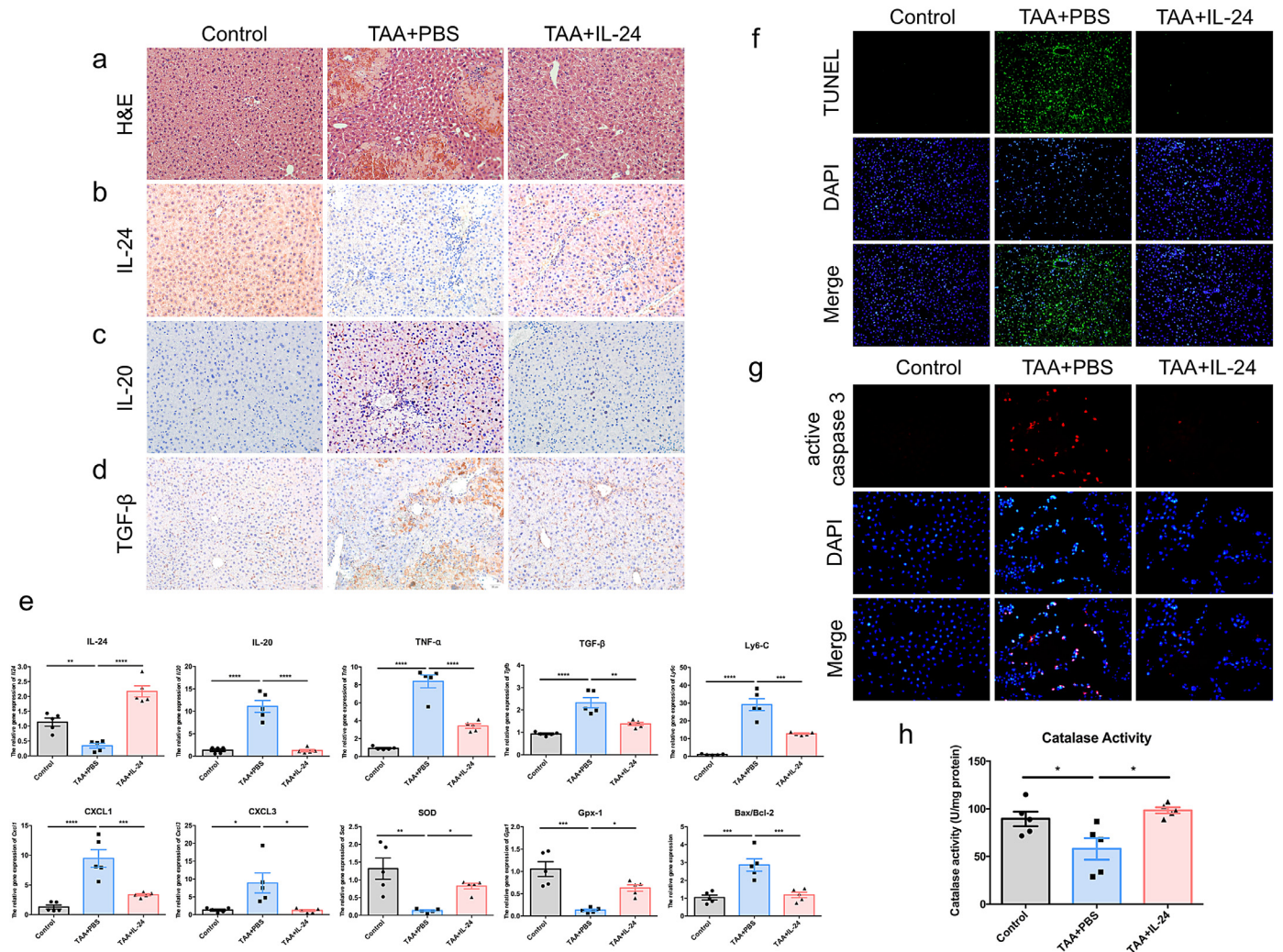
Fig. 2. IL-24 protein protected mice from liver damage in the model of TAA-induced acute liver injury. Mouse IL-24 protein or PBS was intraperitoneally injected into mice 24 h before TAA treatment and 24 h and 48 h after TAA treatment (n = 5 each group). All mice were sacrificed 72 h after TAA treatment. (a) H&E stain was used to analyze the necrosis area. The TAA+IL-24 group had milder damage compared to that of the TAA-alone group. Original magnification: 200 × . (b-d) Immunohistochemistry was used to analyze expression level of IL-24, IL-20, and TGF-β by AEC chromogen stain (red), and the nuclei were counterstained with hematoxylin (blue). Original magnification: 200 × . (e) The mRNA transcripts of *Il24, Il20, Tnfa, Tgfb, Ly6c, Cxcl1, Cxcl3, Sod, Gpx1,* and *Bax/Bcl2* were analyzed using real-time PCR with specific primers. *Gapdh* was used as an internal control. One-way ANOVA, * $p < 0.05$, ** $p < 0.01$, *** $p < 0.001$, **** $p < 0.0001$ compared with TAA+PBS group. Data are means ± SEM. (f) TUNEL assay was used to analyze the apoptotic cells (green) in the liver. Nuclei were stained with DAPI (blue). Original magnification: 100 × . (g) AML12 hepatocytes cell line were treated with deionized water (control) or TAA (100 mM) or TAA+IL-24 (400 ng/ml) for 24 h. Immunofluorescence was used to analyze level of the apoptotic marker-cleaved-caspase 3 (red). Nuclei were stained with DAPI (blue). Original magnification: 200 × . (h) The activity of catalase in the liver was also measured. One-way ANOVA, p = 0.0103. * $p < 0.05$ compared with TAA+PBS group. The experiments in a-h were repeated three times independently with similar results, and the data of one representative experiment was shown.

against liver fibrosis by regulating the activation of HSCs. We analyzed the direct effects of IL-24 on the activation of primary HSCs. Primary HSCs isolated from mice were treated with PBS or IL-24 (400 ng/ml) or IL-20 (400 ng/ml) from day 0 and the culture medium was changed every two days. Immunofluorescence staining showed that IL-24-treated group had less α-SMA stress fiber than the PBS-treated and IL-20-treated group on day 3 (Fig. 4c). The mRNA level of *Acta2* and *Tgfb* were also downregulated by IL-24 on day 7 (Fig. 4d). The results indicated IL-24 specifically targeted HSCs and inhibited its activation. Activated HSCs were characterized by highly proliferating properties. Thus, we also tested whether IL-24 had effects on the proliferation of activated HSCs. IL-24 treatment significantly inhibited the cell proliferation of activated HSC cell line (Fig. 4e). These results demonstrated that IL-24 inhibits the activation and proliferation of HSCs and plays a crucial role in preventing fibrosis.

3.6. IL-24 plays a protective role in HSCs and hepatocytes in an IL-20R1-independent manner

Based on the aforementioned results, although IL-24 and IL-20 interacted with the same receptor complexes (IL-20R1/IL-20R2 or IL-20R2/IL-22R1) on target cells, they seemed to have opposite functions during liver injury. To clarify these two different mechanisms, we analyzed the effects of IL-24 or IL-20 on the isolated primary hepatic stellate cells (HSCs) from wild-type, IL-20R1-, and IL-20R2-deficient mice. The primary HSCs were treated with IL-24 or IL-20 on day 5 after isolation. We harvested the mRNA and analyzed the expression level of *Acta2* on day 7. IL-24 suppressed *Acta2* in both wild-type and IL-20R1-deficient HSCs but not in IL-20R2-deficient HSCs (Fig. 5a). However, IL-20 induced *Acta2* expression only in HSCs from wild-type mice but not from IL-20R1-deficient mice (Fig. 5b). These results indicated that IL-24 inhibits the expression of *Acta2* in
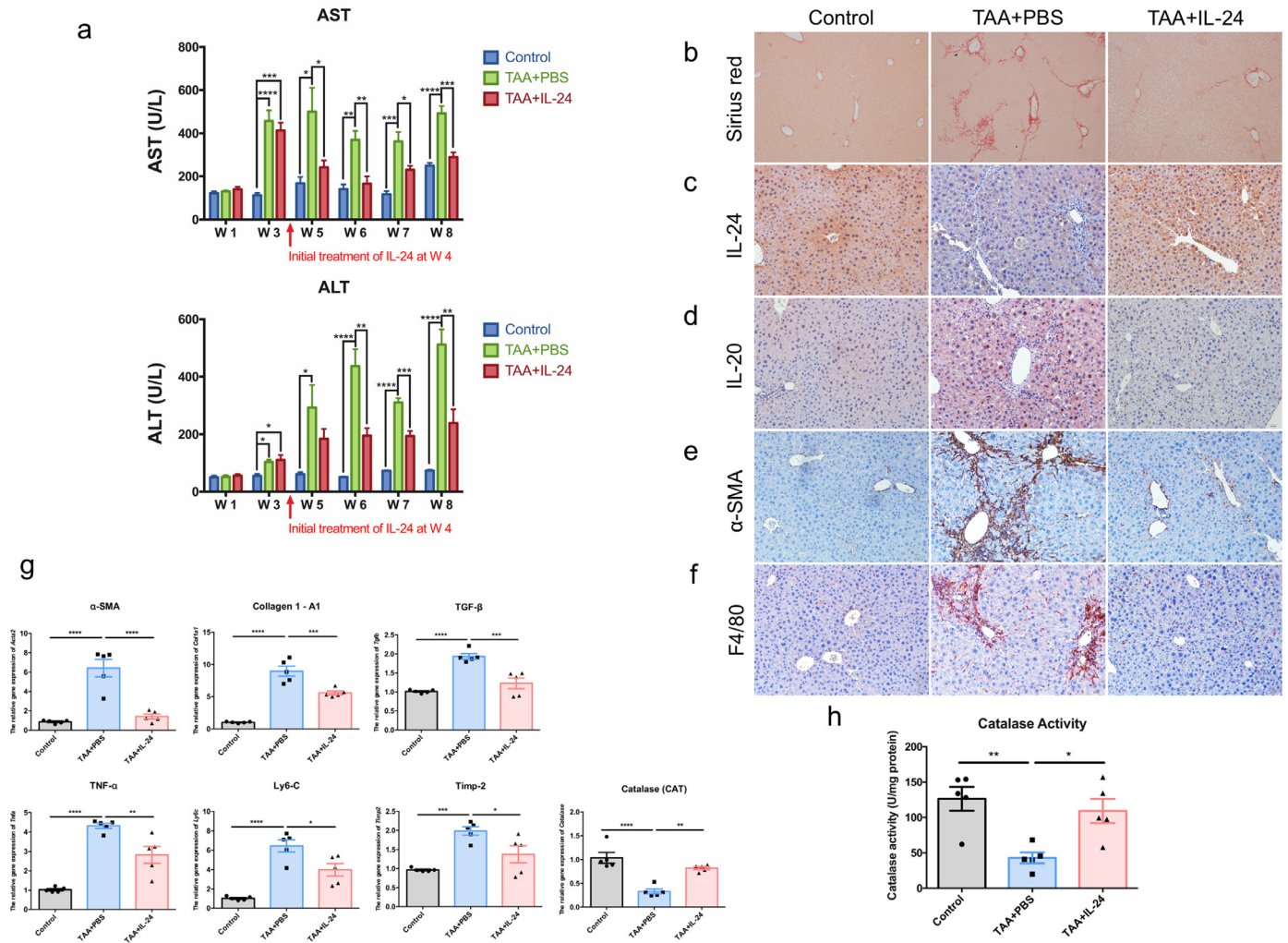
Fig. 3. IL-24 protein-treated mice were resistant to TAA-induced chronic liver injury. Wild-type mice were treated with TAA for 8 weeks to establish long-term liver injury model. Treatment with mouse IL-24 protein (IL-24) was started after 4 weeks of TAA treatment (*n* = 5 each group). (a) Serum levels of aspartate aminotransferase (AST) and alanine amino-transferase (ALT) were analyzed. One-way ANOVA, * $p < 0•05$, ** $p < 0•01$, *** $p < 0•001$, **** $p < 0•0001$ compared with control or TAA+PBS group. (b) Sirius red stain was used to analyze the deposition of collagen. Original magnification: 100 × . (c-f) Immunohistochemistry was used to detect the expression level of IL-24, IL-20, activated HSCs marker − α-SMA, and the liver macrophage marker − F4/80 in chronic liver injury model. The reaction was detected using AEC chromogen stain (red), and the nuclei were counterstained with hematoxylin (blue). Original magnification: 200 × . (g) The mRNA transcripts of *Acta2, Col1a1, Tgfb, Tnfa, Ly6c, Timp2,* and *Cat* were analyzed using real-time PCR with specific primers. *Gapdh* was used as an internal control. One-way ANOVA, * $p < 0•05$, ** $p < 0•01$, *** $p < 0•001$, **** $p < 0•0001$ compared with TAA+PBS group. Data are means ± SEM. (h) The liver catalase activity in different groups was analyzed. One-way ANOVA, $p = 0•0038$; * $p < 0•05$, ** $p < 0•01$ compared with TAA+PBS group. Data are means ± SEM. The experi-ments in b-h were repeated three times independently with similar results, and the data of one representative experiment was shown.

an IL-20R1-independent manner, while IL-20 needs IL-20R1 to induce the activation of HSCs.

Considering the different effects of IL-24 and IL-20 on the growth of activated HSCs, we analyzed the effects of IL-24 or IL-20 on the expression of proliferating cell nuclear antigen (*Pcna*), which is involved in HSCs proliferation. IL-24 suppressed *Pcna* expression in wild-type and IL-20R1-deficient HSCs but not in IL-20R2-deficient HSCs (Fig. 5c). However, IL-20 induced the expression of *Pcna* only in the HSCs from wild-type mice (Fig. 5d). The results indicate that IL-24 suppressed the proliferation of HSCs by inhibiting *Pcna* in an IL-20R1-independent manner. On the contrary, IL-20 induced HSCs pro-liferation primarily through the IL-20R1/IL-20R2 receptor complex.

To further determine whether IL-24 and IL-20 have different effects on hepatocytes, we evaluated the effects of IL-24 or IL-20 on the isolated primary hepatocytes from wild-type, IL-20R1-, and IL-20R2-deficient mice. IL-24 treatment significantly suppressed *Tgfb* in the hepatocytes from wild-type and IL-20R1-deficient mice. How-ever, IL-24 did not affect the expression of *Tgfb* in hepatocytes from IL-20R2-deficient mice owing to the deficiency of both receptor

complexes of IL-24 (Fig. 5e). IL-20 upregulated *Tgfb* only in the hepa-tocytes from wild-type mice but did not affect the hepatocytes from IL-20R1- or IL-20R2-deficient mice (Fig. 5f). These results indicate that IL-20R1 is dispensable for IL-24 to inhibit *Tgfb* expression, while IL-20 needs IL-20R1 to exert a detrimental effect on hepatocytes.

In addition, we used gene knockdown experiments to further study the importance of IL-20R2 and IL-22R1 for IL-24 function. We respectively knocked down IL-20R2 or IL-22R1 of AML12 mouse hepatocyte cell lines, and then added IL-24 or IL-20 to observe the changes in the downstream gene *Col1a1* expression. Western blot was applied to confirm the knockdown efficiency (Figure S11). IL-24 significantly inhibited the gene expression of *Col1a1* in Scramble control but had no influence on *Col1a1* expression in IL-20R2-knockdown and IL-22R1-knockdown cells (Fig. 5g). On the contrary, IL-20 promoted the gene expression of *Col1a1* in Scramble control and IL-22R1 knockdown cells, but not in IL-20R2-knockdown cells (Fig. 5h). The results showed IL-24 and IL-20 preferred to use different receptor complexes to have opposite effects on liver cells.
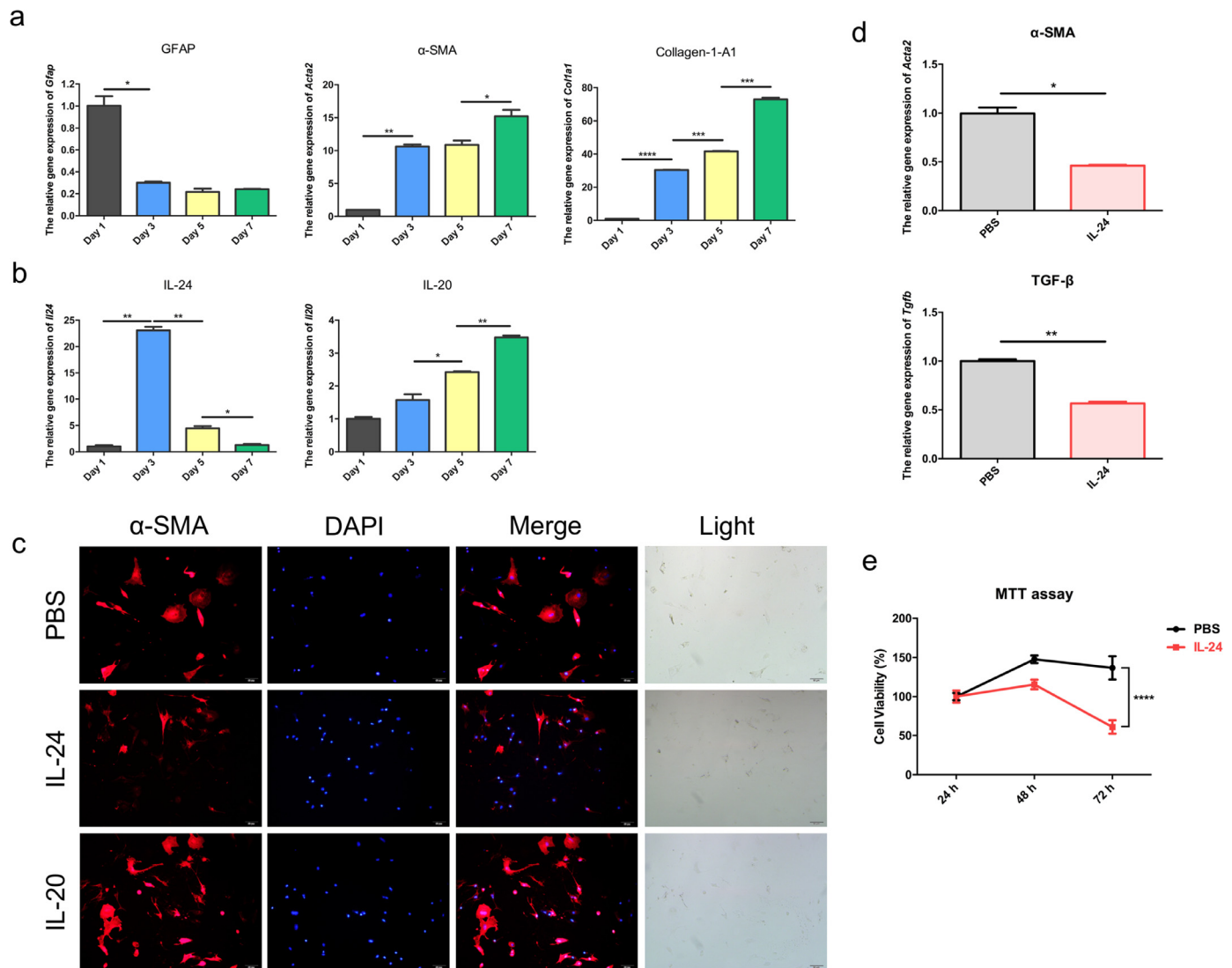
Fig. 4. IL-24 inhibited gene expression of α-SMA in primary HSCs. Primary HSCs were isolated from wild-type mice for cell culture. The mRNA was isolated on day 1, day 3, day 5, and day 7. (a) Real-time PCR was conducted to analyze the gene expression of the quiescent HSCs marker − *Gfap*, the activated HSCs marker − α-SMA (*Acta2*), and alpha-1 type I collagen (*Col1a1*). *Gapdh* was used as an internal control. Two-tailed unpaired *t*-test, * $p < 0 \bullet 05$, ** $p < 0 \bullet 01$, *** $p < 0 \bullet 001$, **** $p < 0 \bullet 0001$. Data are means ± SEM. (b) The gene expression of *Il24* and *Il20* was analyzed by real-time PCR with specific primers. Two-tailed unpaired *t*-test, * $p < 0 \bullet 05$ and ** $p < 0 \bullet 01$. Data are means ± SEM. During the activation of HSCs, the gene expression of *Il24* declined, while the expression of *Il20* was gradually increased. (c) Primary hepatic stellate cells were isolated from mice and were immediately treated with PBS or IL-24 or IL-20 protein. Immunofluorescence was used to determine the protein expression of α-SMA (red) on day 3. Nuclei were stained with DAPI (blue). Original magnification: 200 × . (d) Primary hepatic stellate cells were isolated from mice and were immediately treated with PBS or IL-24 protein. Real-time PCR was applied to analyze the mRNA transcript of *Acta2* and *Tgfb* on day 7. *Gapdh* was used as an internal control. Data are means ± SEM. Two-tailed unpaired *t*-test, * $p < 0 \bullet 05$ and ** $p < 0 \bullet 01$ compared with PBS group. Data are means ± SEM. (e) MTT assay showed the proliferation of the activated HSC at 24, 48 and 72 h. The percentage of cell viability was calculated. Two-tailed unpaired *t*-test, **** $p < 0 \bullet 0001$ compared with PBS group. Data are means ± SEM. The experiments in a-e were repeated three times independently with similar results, and the data of one representative experiment was shown.

3.7. IL-20R2-deficient mice showed severe liver damage in TAA-induced liver injury model

To further confirm that IL-24 protected against liver fibrosis mainly through IL-20R1-independent signaling on liver cells, we induced liver injury in wild-type, IL-20R1-, and IL-20R2-deficient mice. We found IL-20R1-deficient mice have significantly improved liver damage compared to those in the wild-type and IL-20R2-deficient mice (Fig. 6a). It may be because IL-20 cannot effectively perform bad effects due to lack of IL-20R1, and IL-24 can still have protective effects in the absence of IL-20R1. There was a higher bilirubin level in wild-type and IL-20R2-deficient mice after TAA treatment (Fig. 6b). Serum levels of AST and ALT were significantly higher in the wild-type and IL-20R2-deficient mice at 72 h after TAA treatment

(Fig. 6c). The expression levels of genes encoding fibrogenic factor *Tgfb* and chemokine *Cxcl1* (KC) and *Bax/Bcl2* were also upregulated in the livers of the IL-20R2-deficient mice (Fig. 6d). The more severe effects observed in IL-20R2-deficient mice may attribute to the fact that IL-24 is unable to act on liver cells without IL-20R2 to exert protection function.

In the long-term TAA-induced chronic liver injury, long-term carbon tetrachloride (CCl₄)-induced liver injury, and HFD-induced metabolic liver injury models, we also observed that the deficiency of IL-20R2 induced more severe effects in the liver than those in the wild-type mice (Figure S12-S14). Based on these results, we concluded that IL-24 binds to the IL-20R2/IL-22R1 receptor complex on liver cells to protect against liver fibrosis that is independent from IL-20R1.
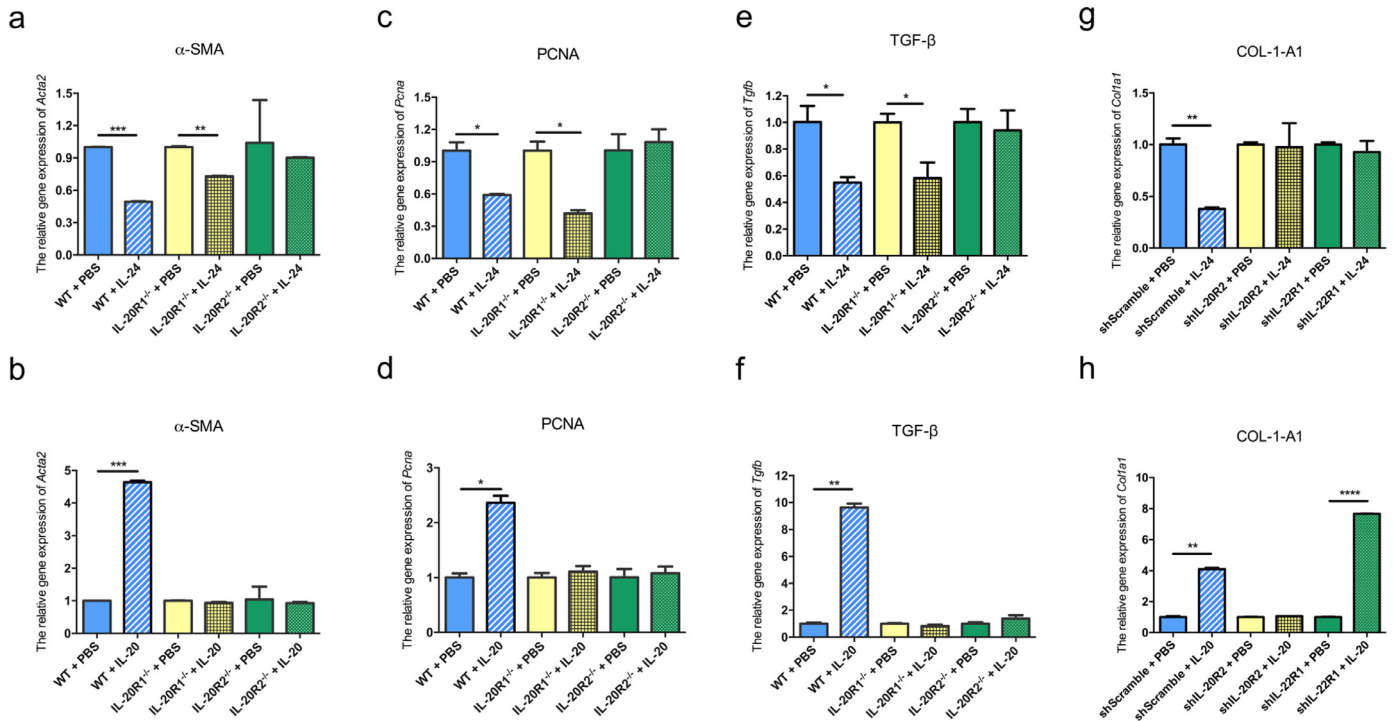
Fig. 5. IL-24 exerted protective effects on HSCs and hepatocytes in an IL-20R1-independent manner. The effects of IL-24 or IL-20 on the isolated primary HSCs from wild-type, IL-20R1-, and IL-20R2- deficient mice were analyzed. (a) Primary HSCs were isolated for cell culture. PBS or IL-24 were added to the cells on day 5. Two days later, mRNA was harvested and was analyzed for the gene expression of the activated HSCs marker − α-SMA (*Acta2*) by real-time PCR with specific primers. *Gapdh* was used as an internal control. Two-tailed unpaired *t*-test, *p* = 0•0002*** between WT+PBS and WT+IL-24, *p* = 0•0012** between IL-20R1KO+PBS and IL-20R1KO+IL-24, *p* = 0•6744 between IL-20R2KO+PBS and IL-20R2KO +IL-24. (b) The effects of IL-20 on the gene expression of *Acta2* was also analyzed. Two-tailed unpaired *t*-test, *p* = 0•0002*** between WT+PBS and WT+IL-20, *p* = 0•0926 between IL-20R1KO+PBS and IL-20R1KO+IL-20, *p* = 0•7326 between IL-20R2KO+PBS and IL-20R2KO+IL-20. (c) The effect of IL-24 on the gene expression of *Pcna* in primary HSCs was analyzed by real-time PCR. Two-tailed unpaired *t*-test, *p* = 0•0329* between WT+PBS and WT+IL-24, *p* = 0•0208* between IL-20R1KO+PBS and IL-20R1KO+IL-24, *p* = 0•5565 between IL-20R2KO+PBS and IL-20R2KO+IL-24. (d) The effects of IL-20 on the gene expression of *Pcna* in primary HSCs. Two-tailed unpaired *t*-test, *p* = 0•0117* between WT+PBS and WT+IL-20, *p* = 0•4168 between IL-20R1KO+PBS and IL-20R1KO+IL-20, *p* = 0•6304 between IL-20R2KO+PBS and IL-20R2KO+IL-20. (e) Primary hepatocytes isolated from WT, IL-20R1-, and IL-20R2-deficient mice were treated with PBS or IL-24 for 8 h. The mRNA transcript of *Tgfb* was analyzed by real-time PCR. Two-tailed unpaired *t*-test, *p* = 0•0373* between WT +PBS and WT+IL-24, *p* = 0•0465* between IL-20R1KO+PBS and IL-20R1KO+IL-24, *p* = 0•6684 between IL-20R2KO+PBS and IL-20R2KO+IL-24. (f) The effects of IL-20 on the gene expression of *Tgfb* were analyzed. Two-tailed unpaired *t*-test, *p* = 0•0012** between WT+PBS and WT+IL-20, *p* = 0•1702 between IL-20R1KO+PBS and IL-20R1KO+IL-20, *p* = 0•1911 between IL-20R2KO+PBS and IL-20R2KO+IL-20. (g) PBS or IL-24 was added to shScramble, shIL-20R2, and shIL-22R1 AML12 mouse hepatocytes cell line for 6 h. The mRNA transcript of *Col1a1* was analyzed by real-time PCR. Two-tailed unpaired *t*-test, *p* = 0•0089** between WT+PBS and WT+IL-24, *p* = 0•05,799 between IL-20R1KO+PBS and IL-20R1KO+IL-24, *p* = 0•9279 between IL-20R2KO+PBS and IL-20R2KO+IL-24. (h) The effects of IL-20 on the expression of *Col1a1* in shScramble, shIL-20R2, and shIL-22R1 AML12 cells were analyzed. Two-tailed unpaired *t*-test, *p* = 0•0012** between WT+PBS and WT+IL-20, *p* = 0•1088 between IL-20R1KO+PBS and IL-20R1KO+IL-20, *p*<0•0001**** between IL-20R2KO+PBS and IL-20R2KO+IL-20. Data are means ± SEM. The experiments in a-h were repeated three times independently with similar results, and the data of one representative experiment was shown.

4. Discussion

Through the analysis of clinical biopsy specimens from patients with liver fibrosis, IL-24 was mainly expressed in non-fibrotic area. While IL-20 was strongly expressed in the activated HSCs-rich fibrotic region. The expression ratio of IL-24 /IL-20 was decreased in patients with more severe liver diseases. It indicated the loss of IL-24 in hepatocytes may cause the fibrosis of the liver and the increased expression of IL-20 may associate with the occurrence of liver fibrosis. Thus, IL-24 has potential to play a protective role in maintaining the liver physiologic homeostasis.

The hepatoprotective effects of IL-24 were evaluated by the acute and chronic liver injury mice models. The same expression patterns of IL-24 and IL-20 were also observed in the mice models. IL-24 was highly expressed in healthy liver tissues. As the liver is damaged by toxins, its expression level decreases significantly, while the expression of IL-20 was increased. IL-24 treatment significantly protected mice against acute and chronic liver injury with reduced liver damage, improved liver function, and suppressed liver inflammation. IL-24 effectively protected hepatocytes from TAA-induced apoptosis both *in vivo* and *in vitro* cell experiments.

Recently, the infiltrating Ly-6C+ monocyte-derived macrophages are linked to chronic inflammation and fibrogenesis [10,23]. Reduced

gene expression of *Ly6c* was observed in the liver after IL-24 treatment, indicating IL-24 may also inhibit the recruitment of Ly6C+ monocyte into the liver to decelerate fibrotic process. Furthermore, IL-20 was downregulated in IL-24-treated mice. In view of the fact that we previously found IL-20 a key deleterious molecule that promotes cell cycle arrest of hepatocytes and the activation of HSCs [19]. These results indicate that IL-24 is an upstream regulator during liver injury and plays a protective role in liver fibrosis.

The dynamic expression of *Il24* and *Il20* in the primary HSCs during activation was also analyzed. *Il24* was initially upregulated but was significantly downregulated upon HSCs activation. However, *Il20* was continuously upregulated during HSCs activation. Therefore, quiescent HSCs had higher *Il24* and lower *Il20* levels than the activated HSCs. Considering the correlation between the activated HSCs and the stage of liver disease [24], these results indicate that IL-24 potentially functions to maintain the properties of quiescent HSCs.

HSCs activation is crucial for the deposition of the ECM during liver fibrosis [25]. We investigated whether IL-24 protects against liver fibrosis by regulating HSCs activation. IL-24 treatment significantly reduced HSCs activation, as evident from the reduction in α-SMA in chronic TAA-induced chronic liver fibrosis model. Using the *in vitro* cell culture of primary HSCs from mice, we found that IL-24 directly inhibited the activation of primary HSCs. Furthermore,
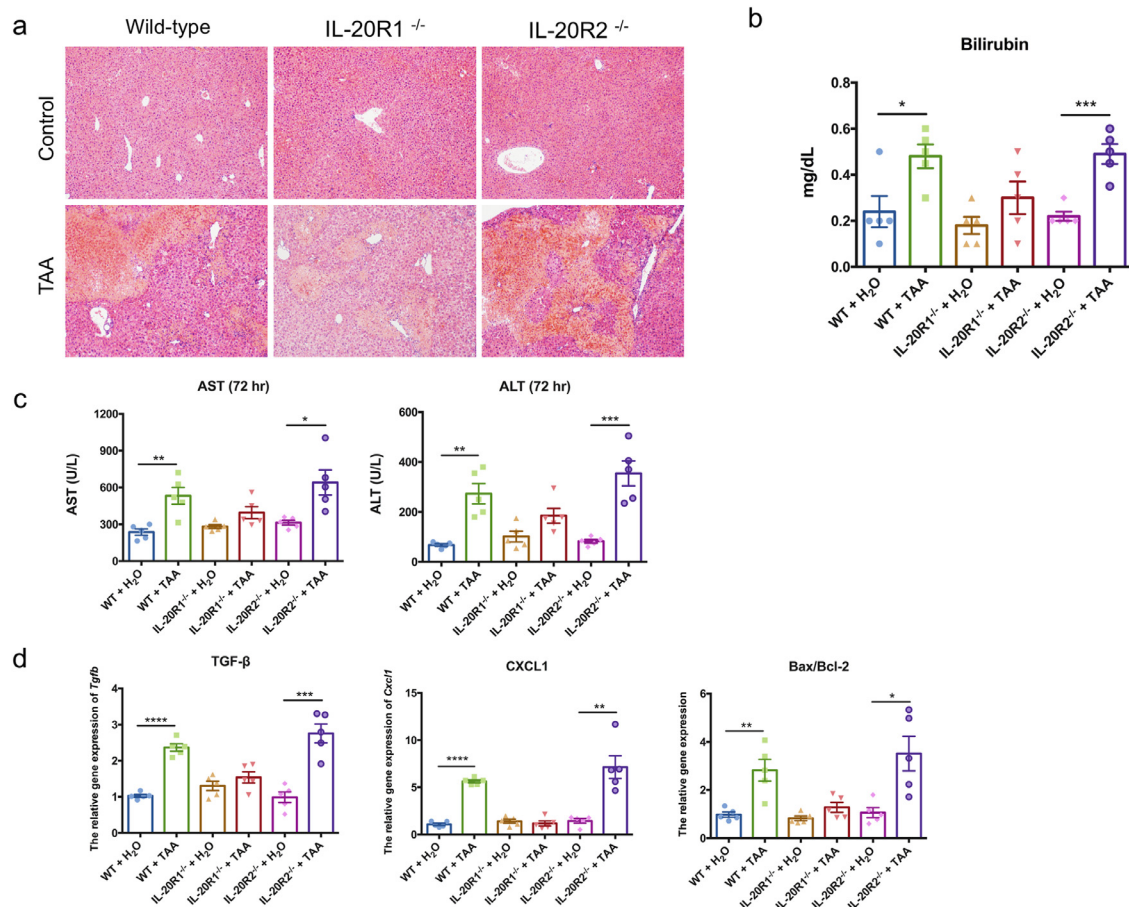
Fig. 6. IL-20R2-deficient (knockout; KO) mice exhibited more severe liver damage than IL-20R1-deficient mice in TAA-induced acute liver injury model. Wild-type, IL-20R1-, and IL-20R2-deficient mice were treated with TAA to induce short-term TAA-induced liver injury (n = 5 each group). (a) H&E stain of mouse liver sections was used to analyze the necrosis area at 72 h after TAA treatment. Original magnification: 100 × . (b) Serum bilirubin was measured at 72 h. Two-tailed unpaired t-test, p = 0•0225* between WT+H$_2$O and WT+TAA, p = 0•1720 between IL-20R1KO+ H$_2$O and IL-20R1KO+TAA, p = 0•0005*** between IL-20R2KO+ H$_2$O and IL-20R2KO+TAA. (c) Serum AST and ALT were measured at 72 h after TAA treatment. Two-tailed unpaired t-test, * p< 0•05, ** p< 0•01, and *** p< 0•001 compared with H$_2$O group. (d) The mRNA expression of *Tgfb, Cxcl1*, and *Bax/Bcl2* in the liver was analyzed using real-time PCR at 72 h after TAA treatment. *Gapdh* was used as an internal control. Two-tailed unpaired t-test, * p< 0•05, ** p< 0•01, *** p< 0•001, and **** p< 0•0001 compared with H$_2$O group. Data are means ± SEM. The experiments in a-d were repeated three times independently with similar results, and the data of one representative experiment was shown.

the proliferation of activated HSCs was also inhibited by IL-24. These results indicate that IL-24 protects against liver fibrosis by specifically inhibiting HSCs activation and proliferation.

Although both IL-24 and IL-20 share the same receptor complexes, they seem to play opposite roles in liver fibrosis. To clarify the detailed mechanism, we analyzed the effects of IL-24 and IL-20 on primary HSCs isolated from wild-type, IL-20R1-, and IL-20R2-deficient mice. The results demonstrated that IL-24 and IL-20 use different receptor complexes to exert opposite effects in the liver. The knockdown experiments further confirmed that IL-24 prefers to use IL-20R2/IL-22R1 to have protective effects on hepatocytes, however, IL-20 exerts harmful effects mainly through IL-20R1/IL-20R2 receptor complex.

IL-24 was believed to bind to cells through IL-20R1/IL-20R2 or IL-20R2/IL-22R1 [26]. Our results showed an increase in gene expression after IL-24 treatment in IL-20R2-deficient cells, which raises the possibility that other unknown receptors may be involved in IL-24 signaling. Whether IL-24 activates signals through other unknown novel receptors awaits further investigation.

To further confirm the different usages of receptor complexes, wild-type, IL-20R1-, and IL-20R2-deficient mice were used to establish several liver injury models. In acute TAA-, chronic TAA-, chronic CCl$_4$-, and high-fat diet- induced liver injury models, IL-20-mediated harmful effects were attenuated by impaired IL-20R1 signaling, as

evidence from the protective effects observed in IL-20R1-deficient mice, which had the same results as our previous publication [19]. In contrast, IL-20R2-deficient mice exhibited more severe liver damage owing to the deficiency of the IL-24-induced protective signaling pathway.

Due to the absence of both IL-20 and IL-24 signaling in IL-20R2-deficient mice, we assumed that the liver damage in IL-20R2-deficient mice would not be more severe than that in wild-type mice. We were surprised to find that IL-20R2-deficient mice exhibited more severe liver damage than wild-type mice in response to long-term TAA, long-term CCl$_4$ and high fat diet treatment. These results suggested that other factors, which bind to IL-20R2, might also be involved in the liver injury. IL-19, another member of the IL-10 family, which also binds to the IL-20R1/IL-20R2 receptor complex on target cells may be involved in the liver fibrosis [16]. However, the exact function of IL-19 in liver injury requires further clarification.

Along with IL-24 and IL-20, IL-22 was also involved in liver fibrosis [27]. However, the results are controversial. For instance, IL-22 promotes liver fibrosis by regulating TGF-β and activating HSCs [28,29]. In contrast, IL-22 plays a protective role through anti-fibrotic functions and promotion of regeneration [30-32]. It awaits further investigation whether a regulatory link exists between IL-24 and IL-22.

In recent years, there have been several studies on the potential therapeutic applications of IL-24, most of them focused on the

protective role of IL-24 in cancers. The beneficial functions of IL-24 include inducing apoptosis, antitumor activity, and anti-angiogenic properties in various cancer cells [33]. IL-24 effectively inhibits the growth and metastasis of hepatoma cells [27,34]. The therapeutic strategy combining IL-24 gene therapy and the use of chemotherapy drugs is an efficient method of killing certain types of cancer cells [35]. In addition, IL-24 has proven efficacious in phase I/II clinical trials in humans with multiple advanced cancers [36].

Hepatic fibrosis is a wound healing response that follows chronic liver damage, eventually leading to cirrhosis. Until now, liver transplantation has been the only treatment option for advanced fibrosis and cirrhosis [37]. Thus, the development of effective anti-fibrotic drugs could greatly improve the treatment of this serious disease. Our results demonstrate that IL-24 is a promising hepatoprotective cytokine with several characteristics: (1) In patients with lower IL-24 protein level, the fibrosis score and METAVIR score is higher. The protein expression ratio of IL-24/IL20 was decreased with patients with more severe liver diseases. (2) IL-24 protects mice from toxin-induced acute and chronic liver injury by reducing the area of the damaged liver, improving liver function, and suppressing liver inflammation. (3) IL-24 is a potent anti-fibrotic factor by regulating several pro-fibrotic gene expression on liver cells. (4) IL-24 not only protected hepatocytes from toxin-induced apoptosis but also inhibited the activation and proliferation of the HSCs. Here, we revealed the significant protection of IL-24 in the liver injury process. In conclusion, our results demonstrated a novel function of IL-24 and provided a potential therapeutic candidate for the treatment of liver fibrosis.

Contributors

HHW, JHH, MHS, and WCH conducted the literature search and designed animal and cell experiments. HHW and JHH were responsible for data collection, analysis, and data interpretation. HHW, YHH, and MSC wrote the manuscript. KCC helped with the IHC staining and pathologic analysis of liver tissue. HHW, JHH, and YHH had verified the underlying data. MSC and YHH coordinated and directed the entire project. All authors read and approved the final manuscript.

Abbreviations

7E: anti$-$IL$-$20 monoclonal antibody, $\alpha-$SMA: alpha$-$smooth$-$muscle actin, ALT: alanine aminotransferase, AST: aspartate aminotransferase, CCl$_4$: carbon tetrachloride, COL-1-A1: alpha-1 type I collagen, ECM: extracellular matrix, HCC: hepatocellular carcinoma, HFD: high-fat diet, HSCs: hepatic stellate cells, IL: interleukin, TAA: thioacetamide, TGF-β: transforming growth factor-β, TIMPs: tissue inhibitors of metalloproteinases, TNF-α: tumor necrosis factor-α

Declaration of Competing Interest

The authors declare no conflicts of interest.

Acknowledgments

Data sharing statement

The data that support the findings of this study are available from the corresponding author, Ming-Shi Chang upon reasonable request.

Supplementary materials

Supplementary material associated with this article can be found in the online version at doi:10.1016/j.ebiom.2021.103213.

References

[1] Arriazu E, Ruiz de Galarreta M, Cubero FJ, Varela-Rey M, Perez de Obanos MP, Leung TM, et al. Extracellular matrix and liver disease. Antioxid Redox Signal 2014;21(7):1078–97.

[2] Parola M, Pinzani M. Liver fibrosis: pathophysiology, pathogenetic targets and clinical issues. Mol Aspects Med 2019;65:37–55.

[3] Van de Bovenkamp M, Groothuis GM, Meijer DK, Olinga P. Liver fibrosis in vitro: cell culture models and precision-cut liver slices. Toxicol In Vitro 2007;21 (4):545–57.

[4] Bataller R, Brenner DA. Liver fibrosis. J Clin Invest 2005;115(2):209–18.

[5] Fabregat I, Moreno-Caceres J, Sanchez A, Dooley S, Dewidar B, Giannelli G, et al. TGF-beta signalling and liver disease. FEBS J 2016;283(12):2219–32.

[6] Friedman SL. Liver fibrosis – from bench to bedside. J Hepatol 2003;38(Suppl 1): S38–53.

[7] Zhang CY, Yuan WG, He P, Lei JH, Wang CX. Liver fibrosis and hepatic stellate cells: etiology, pathological hallmarks and therapeutic targets. World J Gastroenterol 2016;22(48):10512–22.

[8] Lee UE, Friedman SL. Mechanisms of hepatic fibrogenesis. Best Pract Res Clin Gastroenterol 2011;25(2):195–206.

[9] Heymann F, Trautwein C, Tacke F. Monocytes and macrophages as cellular targets in liver fibrosis. Inflamm Allergy Drug Targets 2009;8(4):307–18.

[10] Tacke F, Zimmermann HW. Macrophage heterogeneity in liver injury and fibrosis. J Hepatol 2014;60(5):1090–6.

[11] Dewidar B, Meyer C, Dooley S, Meindl-Beinker AN. TGF-beta in Hepatic Stellate Cell Activation and Liver Fibrogenesis-Updated 2019. Cells 2019;8(11):1419.

[12] Dong X, Liu J, Xu Y, Cao H. Role of macrophages in experimental liver injury and repair in mice. Exp Ther Med 2019;17(5):3835–47.

[13] Xu J, Liu X, Koyama Y, Wang P, Lan T, Kim IG, et al. The types of hepatic myofibroblasts contributing to liver fibrosis of different etiologies. Front Pharmacol 2014;5:167.

[14] Elpek GO. Cellular and molecular mechanisms in the pathogenesis of liver fibrosis: an update. World J Gastroenterol 2014;20(23):7260–76.

[15] Tsuchida T, Friedman SL. Mechanisms of hepatic stellate cell activation. Nat Rev Gastroenterol Hepatol 2017;14(7):397–411.

[16] Rutz S, Wang X, Ouyang W. The IL-20 subfamily of cytokines$-$from host defence to tissue homeostasis. Nat Rev Immunol 2014;14(12):783–95.

[17] Wang M, Tan Z, Zhang R, Kotenko SV, Liang P. Interleukin 24 (MDA-7/MOB-5) signals through two heterodimeric receptors, IL-22R1/IL-20R2 and IL-20R1/IL-20R2. J Biol Chem 2002;277(9):7341–7.

[18] Chen J, Caspi RR, Chong WP. IL-20 receptor cytokines in autoimmune diseases. J Leukoc Biol 2018;104(5):953–9.

[19] Chiu YS, Wei CC, Lin YJ, Hsu YH, Chang MS. IL-20 and IL-20R1 antibodies protect against liver fibrosis. Hepatology 2014;60(3):1003–14.

[20] Wei CC, Chen WY, Wang YC, Chen PJ, Lee JY, Wong TW, et al. Detection of IL-20 and its receptors on psoriatic skin. Clin Immunol 2005;117(1):65–72.

[21] Maschmeyer P., Flach M., Winau F. Seven steps to stellate cells. J Vis Exp. 2011 (51).

[22] Mueller S, Riedel HD, Stremmel W. Determination of catalase activity at physiological hydrogen peroxide concentrations. Anal Biochem 1997;245 (1):55–60.

[23] van der Heide D, Weiskirchen R, Bansal R. Therapeutic targeting of hepatic macrophages for the treatment of liver diseases. Front Immunol 2019;10:2852.

[24] Ionescu AG, Streba LA, Vere CC, Ciurea ME, Streba CT, Ionescu M, et al. Histopathological and immunohistochemical study of hepatic stellate cells in patients with viral C chronic liver disease. Rom J Morphol Embryol 2013;54 (4):983–91.

[25] Hou W, Syn WK. Role of metabolism in hepatic stellate cell activation and fibrogenesis. Front Cell Dev Biol 2018;6:150.

[26] Wang M, Liang P. Interleukin-24 and its receptors. Immunology 2005;114 (2):166–70.

[27] Caparros E, Frances R. The interleukin-20 cytokine family in liver disease. Front Immunol 2018;9:1155.

[28] Fabre T, Molina MF, Soucy G, Goulet JP, Willems B, Villeneuve JP, et al. Type 3 cytokines IL-17A and IL-22 drive TGF-beta-dependent liver fibrosis. Sci Immunol 2018;3(28).

[29] Wu LY, Liu S, Liu Y, Guo C, Li H, Li W, et al. Up-regulation of interleukin-22 mediates liver fibrosis via activating hepatic stellate cells in patients with hepatitis C. Clin Immunol 2015;158(1):77–87.

[30] Khawar MB, Azam F, Sheikh N, Abdul Mujeeb K. How does interleukin-22 mediate liver regeneration and prevent injury and fibrosis? J Immunol Res 2016;2016:2148129.

[31] Pan CX, Tang J, Wang XY, Wu FR, Ge JF, Chen FH. Role of interleukin-22 in liver diseases. Inflamm Res 2014;63(7):519–25.

[32] Kong X, Feng D, Mathews S, Gao B. Hepatoprotective and anti-fibrotic functions of interleukin-22: therapeutic potential for the treatment of alcoholic liver disease. J Gastroenterol Hepatol 2013;28(Suppl 1):56–60.

[33] Fisher PB, Gopalkrishnan RV, Chada S, Ramesh R, Grimm EA, Rosenfeld MR, et al. mda-7/IL-24, a novel cancer selective apoptosis inducing cytokine gene: from the laboratory into the clinic. Cancer Biol Ther 2003;2(4 Suppl 1):S23–37.

[34] Chen WY, Cheng YT, Lei HY, Chang CP, Wang CW, Chang MS. IL-24 inhibits the growth of hepatoma cells *in vivo*. Genes Immun 2005;6(6):493–9.

[35] Inoue S, Shanker M, Miyahara R, Gopalan B, Patel S, Oida Y, et al. MDA-7/IL-24-based cancer gene therapy: translation from the laboratory to the clinic. Curr Gene Ther 2006;6(1):73–91.

[36] Menezes ME, Bhatia S, Bhoopathi P, Das SK, Emdad L, Dasgupta S, et al. MDA-7/IL-24: multifunctional cancer killing cytokine. Adv Exp Med Biol 2014;818:127–53.

[37] Schuppan D, Afdhal NH. Liver cirrhosis. Lancet 2008;371(9615):838–51.